AGU PUBLICATIONS

Tectonics

RESEARCH ARTICLE
10.1002/2017TC004851

Special Section:
Geodynamics, Crustal and Lithospheric Tectonics, and active deformation in the Mediterranean Regions (A tribute to Prof. Renato Funiciello)

Three-Dimensional Modeling of Mount Etna Volcano: Volume Assessment, Trend of Eruption Rates, and Geodynamic Significance

Giovanni Barreca[1], **Stefano Branca**[2], **and Carmelo Monaco**[1]

[1]Dipartimento di Scienze Biologiche, Geologiche e Ambientali, Sezione di Scienze della Terra, Università di Catania, Catania, Italy, [2]Istituto Nazionale di Geofisica e Vulcanologia, Osservatorio Etneo-Sezione di Catania, Catania, Italy

Abstract 3-D modeling of Mount Etna, the largest and most active volcano in Europe, has for the first time enabled acquiring new information on the volumes of products emitted during the volcanic phases that have formed Mount Etna and particularly during the last 60 ka, an issue previously not fully addressed. Volumes emitted over time allow determining the trend of eruption rates during the volcano's lifetime, also highlighting a drastic increase of emitted products in the last 15 ka. The comparison of Mount Etna's eruption rates with those of other volcanic systems in different geodynamic frameworks worldwide revealed that since 60 ka ago, eruption rates have reached a value near to that of oceanic-arc volcanic systems, although Mount Etna is considered a continental rift strato-volcano. This finding agrees well with previous studies on a possible transition of Mount Etna's magmatic source from plume-related to island-arc related. As suggested by tomographic studies, trench-parallel breakoff of the Ionian slab has occurred north of Mount Etna. Slab gateway formation right between the Aeolian magmatic province and the Mount Etna area probably induced a previously softened and fluid-enriched suprasubduction mantle wedge to flow toward the volcano with consequent magmatic source mixing.

Key Points:
- We performed a 3-D modeling of Mount Etna volcano
- Volumes of volcanic phases forming Mount Etna and eruption rates were derived
- Anomalously high eruption rate since 60 ka was related to a significant geodynamic change in the area

Correspondence to:
G. Barreca,
g.barreca@unict.it

Citation:
Barreca, G., Branca, S., & Monaco, C. (2018). Three-dimensional modeling of Mount Etna volcano: Volume assessment, trend of eruption rates, and geodynamic significance. *Tectonics*, *37*. https://doi.org/10.1002/2017TC004851

Received 11 OCT 2017
Accepted 15 FEB 2018
Accepted article online 21 FEB 2018

1. Introduction

Mount Etna in eastern Sicily (Italy) is one of the most active volcanoes in the world and one of the most monitored due to its frequent activity in a densely populated area. It is located at the suture zone between two colliding plates, the European to the north and the African to the south (Figure 1a), along an area currently affected by oblique tectonics resulting from the southeastward shifting of the Calabrian Arc (Palano et al., 2012, and reference therein). The origin of volcanism in the Etnean region is currently best explained through a deep tearing in the lithosphere occurring at the south-western edge of the Ionian/Calabrian subduction zone, which formed as result of the differential retreat of the Ionian slab (Doglioni et al., 2001; Nicolich et al., 2000; Figure 1a). The tearing process favored the passive upwelling of the asthenospheric mantle that melted as consequence of adiabatic decompression (Gvirtzman & Nur, 1999). Although Mount Etna volcanism is near coeval with that of the Aeolian arc (Figure 1a), its Na-alkaline geochemical composition is entirely different from the calc-alkaline to shoshonitic signature of the products of the Aeolian Islands (Peccerillo, 2005a). This is because the two magmatic systems are located in different geodynamic contexts and are fed by melts coming from different mantle sources. Nevertheless, a transition from a predominantly mantle-plume source (rift-related) to an island arc-type source (subduction-related) has occurred at Mount Etna as a consequence of magmatic source mixing (Schiano et al., 2001; Tonarini et al., 2001).

The eruptive activity of Mount Etna is one of the most studied and best documented for any volcano. Extensive field mapping and radiometric dating performed in the last decades (Branca et al., 2011; Branca, Coltelli, & Groppelli, 2011; De Beni et al., 2011, and references therein) have allowed defining a detailed reconstruction of the geological evolution of the volcano. Four main eruptive phases have been recognized by these authors, comprising different volcanic successions related to well-defined periods in which the eruptions occurred with similar eruptive style in the same geodynamic setting. During each phase, several volcanic centers formed and remnants of these are still recognizable in the field.

Mount Etna volcano rests on a sedimentary basement mainly formed by Miocene turbiditic deposits of the Apenninic-Maghrebian chain and by Quaternary foredeep clays (Branca, Coltelli, Groppelli, & Lentini, 2011). The morphological setting of the basement below Etna volcano was reconstructed by several authors through geophysical data (Aureli, 1973; Aureli & Musarra, 1975; Lo Giudice et al., 1981; Monaco et al., 2010;

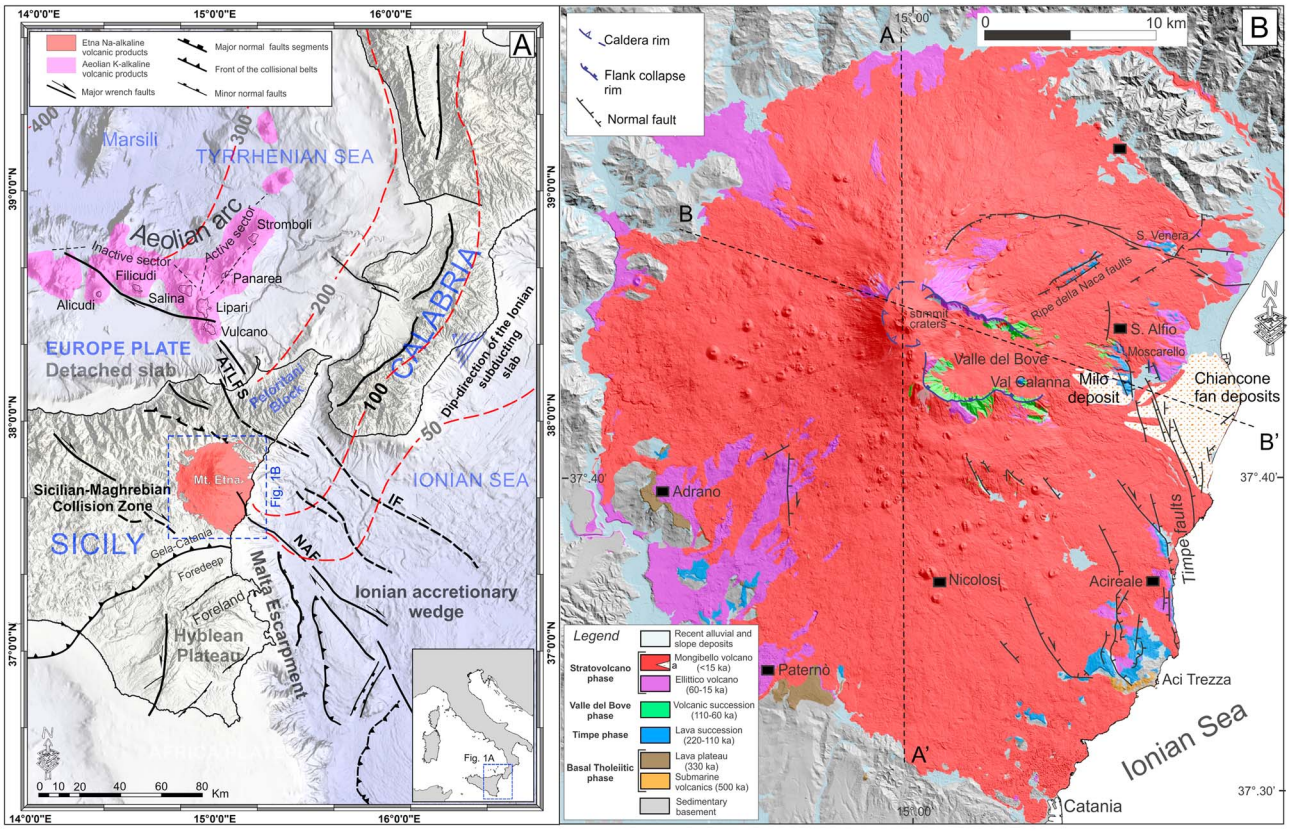

Figure 1. (a) Location of Mount Etna volcano in the geodynamic framework of the eastern Mediterranean (eastern Sicily-Calabrian arc). The shaded-relief basemap is a combination of Emodnet bathymetry (http://www.emodnet-bathymetry.eu) and SRTM 30 plus topography (Shuttle Radar Tomography Mission, http://topex.ucsd.edu/WWW_html/srtm30_plus.html). The volcano is located about 100 km south of the subduction-related Aeolian volcanic arc, and it is thought to sit atop a lithospheric scale fault at the edge of the subducting Ionian slab (Doglioni et al., 2001; Gutscher et al., 2016; Gvirtzman & Nur, 1999). The red dashed lines represent the Benioff-Wadati contours of the slab (Sartori, 2003). Slab edge deformation is expressed by an array of NW-SE trending oblique faults running from the southern Tyrrhenian Sea (ATLFS-Aeolian-Tindari-Letojanni Fault System, see Barreca et al., 2014, 2016; Cultrera et al., 2016) to the Ionian offshore (IF, Ionian Fault; NAF, North Alfeo Fault; see Gutscher et al., 2016; Polonia et al., 2016).,. (b) Geological and structural sketch map of the Etna volcano (modified from Branca, Coltelli, Groppelli, & Lentini, 2011) showing the distribution of volcanic products erupted during the main volcanic phases (a) Milo and Chiancone volcaniclastic deposits. Dashed lines (A-A′ and B-B′) represent the traces of cross sections used to construct the 3-D model.

Ogniben, 1966; Patella & Quarto, 1987; Rust & Neri, 1996). This data allowed Neri and Rossi (2002) to estimate a total volume for Mount Etna volcanic edifice of 374 km^3, obtaining an average eruptive rate of 0.0012 km^3/a for the past 300 ka. Similar total volumes (350 km^3) of the volcanic pile were estimated by Tanguy, Condomines, and Kieffer (1997) and Tanguy (1980) and by Catalano et al. (2004) (about 373 km^3) through the reconstruction of the subvolcanic morphology along a few cross sections. Recently, Branca and Ferrara (2013) have reinterpreted more than 2,500 subsurface data, consisting of geoelectric and borehole prospecting that reached the substratum, thereby reconstructing a detailed contour map of the sedimentary basement. The authors, based on the average thickness and areal distribution of the volcanic products, determined a total volume for Mount Etna of 532 ± 85 km^3 that was emplaced during the past 330 ka, resulting in an average rate of volcanic output of 1.6×10^{-3} km^3/a.

In detail, they obtained volumes for Timpe (93 km^3), Valle del Bove (145 km^3), and stratovolcano (289 km^3) phases, so deriving eruption rates of 8.4×10^{-4}, 2.9×10^{-3}, and 4.8×10^{-3} km^3/a, respectively.

The reconstruction of the temporal variation of the average eruptive rate highlights a drastic increase of volcanism during the last 100 ka. This increase was related to the gradual stabilization of the plumbing system in the Mount Etna region that led to the buildup of the composite stratovolcano structure. Further, Branca and Ferrara (2013) correlated the stratigraphy of the several geognostic continuous corings reaching the sedimentary basement, mainly located on the middle-lower slope of the volcano, with the stratigraphic setting

of the new geological map of Mount Etna volcano (Branca, Coltelli, Groppelli, & Lentini, 2011). This resulted in redefining the entire geological framework of the volcanic pile. It has led to a more precise spatial location of the buried volcanic successions, related to the distinct evolutionary phases, and enabled reassessing the relationships with the morphological setting of the sedimentary basement.

Starting from published data on the relations between the several volcanic centers forming Mount Etna (i.e., geological maps, well-calibrated cross sections, contour maps, and digital terrain model [DTM]), we present a 3-D geological model of the volcano as a result of digital reconstruction of their geometry. All data were managed by using a geomodeling software to generate a volumetric model for the entire volcano, which allows redefining both total and partial (i.e., of the single eruptive phases and volcanic centers) volumes of Mount Etna. Volume-based measurements also enable recalculating time-averaged eruption rates for each considered eruptive phase in the time interval 330 ka to present day and particularly for the last 60 ka. The anomalously high eruption rate during this period has been related to a significant geodynamic change in the area.

2. Geological Setting of Mount Etna

Mount Etna is a late Quaternary polygenic volcano located between the Gela-Catania foredeep and the frontal nappes of the Sicilian-Maghrebian collision zone (Figure 1a). The volcanic edifice has grown within an intricate geodynamic framework, and its activity is believed related to the occurrence of a regional-scale tectonic boundary extending from the central sector of the Aeolian archipelago to the Ionian coast of Sicily (the Aeolian-Tindari-Letojanni fault system, Palano et al., 2012), probably joining to offshore fault systems (e.g., the Malta escarpment, Nicolich et al., 2000; the North Alfeo Fault, Gutscher et al., 2016; and the Alfeo-Etna and/or Ionian Fault, Polonia et al., 2016; see Figure 1a). This major boundary accommodates the lithospheric tearing of the south-western edge of the Ionian slab subducting beneath the Calabrian Arc and the Tyrrhenian basin, whose detachment favored the progressive south-eastward migration of the Calabrian Arc (Govers & Wortel, 2005; Neri et al., 2012). Accordingly, in the last 500 ka, crustal faulting and associated fracturing favored magma ascent through the lithosphere along the Ionian coast of Sicily where volcanic products have accumulated above a Neogene-Quaternary sedimentary clayey basement to form a composite stratovolcano.

According to the new geological investigation made by Branca et al. (2008, 2011b) and geochronological data (De Beni et al., 2011) (Figure 1b), Mount Etna's evolution is divided into four main phases. The oldest phase, named "Basal Tholeiitic," started about 500 ka ago and was characterized during its early stage by discontinuous and scattered submarine eruptive activity. After a long hiatus, during which regional uplift produced the gradual emergence of the early-middle Pleistocene sedimentary basement (Di Stefano & Branca, 2002), the eruptive activity renewed (~330 ka ago) through fissure-type eruptions in a subaerial environment. The superposition of lava flows gave rise to a gentle topography with a wide and thin lava plateau extending for more than 25 km along the western periphery of the volcanic edifice.

Between 220 and 121 ka ago, the "Timpe" phase fissure-type eruptions along the Ionian coast built a primitive volcano structure consisting of a NNW-SSE elongated lava-shield. This is currently exposed along the Timpe system and the Ripe della Naca fault scarps (Figure 1b for location), whereas its southeastern portion lies below sea level down to 660 m deep in the Ionian Sea (Chiocci et al., 2011). In this time span, scattered effusive eruptions also took place in a wide area corresponding to the present-day lower SW and SE flanks of Etna up to about 110 ka. Since 129 ka ago (De Beni et al., 2011), the eruptive activity shifted westward and concentrated in today's Val Calanna area (Nicolosi et al., 2016). Between at least 110 ka and 60 ka, the shifting of magma sources toward the present Valle del Bove area (see Figure 1b for location) marks the beginning of the central-type volcanism with the formation of several small polygenic volcanic centers. This third phase, named "Valle del Bove," was characterized by explosive and effusive activity that led to the buildup of the earlier stratovolcano structure that reached a maximum elevation of about 2600 m (Branca, Coltelli, & Groppelli, 2011). Finally, the "Stratovolcano" phase includes the products of Ellittico and Mongibello volcanoes, erupted during the last 60 ka. In particular, the Ellittico volcano activity began about 60 ka ago, 4 km northwestward of the previous eruptive centers. This volcano reached a maximum elevation of about 3,600 m and was characterized by both explosive and effusive activity from summit vents and flank fissures that favored the emplacement of wide lava flow fields, gradually expanding on the sedimentary basement. The explosive activity produced several thick pyroclastic flow and fall deposits, mainly distributed on the

lower east and west flanks. The Ellittico volcano activity ended between 15 and 15.5 ka ago with several Plinian eruptions (Coltelli et al., 2000; Kieffer, 1979) that formed a wide summit caldera and the deposition of widespread pyroclastic deposits on the eastern flank and in the Mediterranean area (Albert et al., 2013; Coltelli et al., 2000; Del Carlo et al., 2017).

The eruptive activity of the last 15 ka, related to the Mongibello volcano, produced a thick succession consisting of superposed simple and compound lava flows and a pyroclastic successions generated by several strombolian to subplinian events (Coltelli et al., 2000). Around 10 ka, gravitational slope failures involved a large portion of the eastern flank of the volcano, producing the wide depression of the Valle del Bove (Calvari et al., 2004; Figure 1b). The associated volcaniclastic deposits outcrop immediately eastward of the Valle del Bove down to the coast and consist of a debris avalanche deposit and detritic-alluvial body (Branca, Coltelli, Groppelli, & Lentini, 2011; Calvari & Groppelli, 1996; Calvari, Tanner, & Groppelli, 1998).

3. 3-D Model Set Up: Data and Methods

To build the model, we used a pseudo 3-D -modeling approach and procedure (Cristallini & Allmendinger, 2001; Wilkerson et al., 1991), consisting of creating 3-D surfaces by a linear interpolating of reference control lines picked along digital cross-sections and surfaces. All the 3-D features were generated and managed into the Move 2016 geo-modeling software package (Midland Valley Ltd).

Multisource data, including cross sections, geological maps and available contour maps, and digital surfaces, from previously published papers and related data sets, were used to generate the 3-D model of Mount Etna (Figure 2). Cross sections are taken from a recently published work (Branca & Ferrara, 2013) and consist of two N-S and WNW-ESE oriented geological transects along which the top and base contacts of the volcanic edifices are represented (Figure 2a). Available geological maps (e.g., Branca, Coltelli, Groppelli, & Lentini, 2011) provide the areal distribution of the single volcanic edifices (i.e., Valle del Bove, Ellittico, and Mongibello) from which the relative outcrop boundaries were extracted (Figure 2b1–3), whereas buried edges have been reconstructed by correlating outcrop data, as in the case of the eastern limit of the Ellittico edifice (see Figure 2b-2). The morphological shape of the eruptive centers of the Valle del Bove edifice was instead directly derived from the 3-D model by the intersection of its top surface with the grid of sedimentary substratum (Figure 2b-1). The polygons of both reconstructed and outcropping edges have been suitably generalized by using node reduction and smoothing techniques operated into ArcGis platform. Contour maps include the top of the sedimentary basement at 50 m equidistance, as reconstructed by Branca and Ferrara (2013) (Figure 2c), and two other minor schematic representations of the paleo-morphology of the summit area of the Ellittico (Figure 2d-1) and of the Valle del Bove (Figure 2d-1) volcanic edifices. These have been reconstructed by flank dipping data from Branca, Coltelli, Groppelli, and Lentini (2011) and released at lines spaced 200 m. Finally, we used a 10×10 m grid size resolution digital elevation model (DEM) to acquire modern altitude topographic information (Figure 2e).

As a whole, well-calibrated geological profiles represent suitable raw data, and thus, they have been chosen as reference objects around which our 3-D geological model has been constructed.

Since most of the data lack precise spatial references, before starting geomodeling, it was necessary to georeference them. Accordingly, both raster and vector format data were combined and organized in a common coordinate system, the WGS84 Spheroid UTM projection. Surface map objects were georeferenced into ArcGIS with the help of the DEM, which highlights the 2-D spatial relationships between different sets of data. In order to add georeferencing quality control, map objects (e.g., the geological map and other raster images) were draped onto the DEM to help position the cross sections with respect to the surface geology and topography. The images of cross sections were instead converted to 3-D objects directly into Move 2-D module using as spatial domain the coordinates at tips of their traces and the relative z domain (Figure 3a). Georeferenced surface map data and cross sections were therefore integrated by combining them in 3-D Move, exchanging the data between the 2-D and the 3-D environment.

Within the 3-D environment, the features of interest, that is, lithological interfaces in the cross sections and boundaries in surface maps (including outcropping and interpolated), were picked into Move software as 3-D vector objects along the cross sections or reference grid surfaces (e.g., the grid surface of sedimentary substratum). 3-D control lines constituted the backbone of the model through which top and bottom

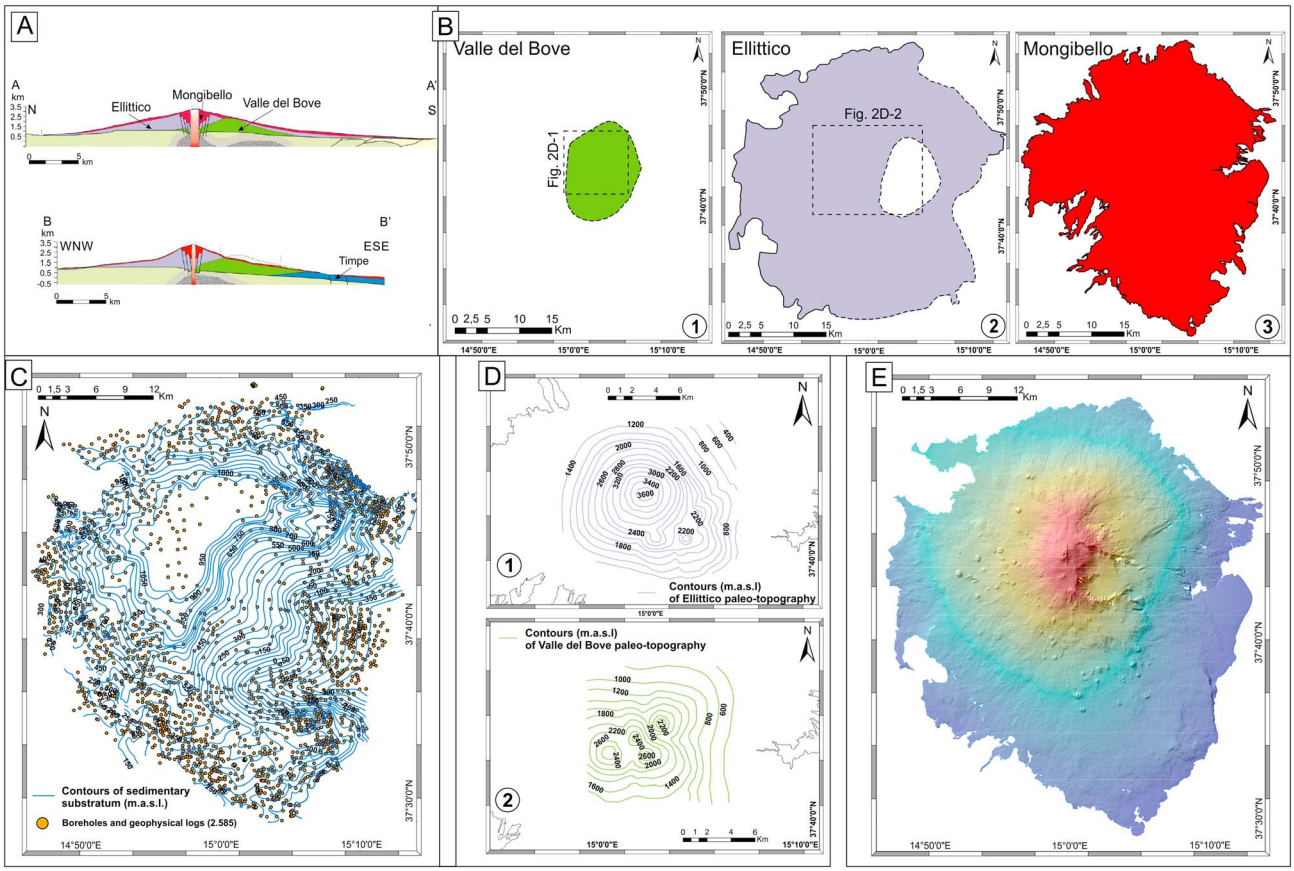

Figure 2. Source data used for the 3-D reconstruction of Mount Etna and related volcanic phases. (a) Well-calibrated cross sections (Branca & Ferrara, 2013; see Figure 1Bb for location), which display the geometric relationships between the distinct volcanic edifices formed during the main volcanic phases of Mount Etna (i.e., Timpe, Valle del Bove, and Stratovolcano). (b) Construction lines used to build up the backbone of the 3-D model: (1) basal boundary of the Valle del Bove edifice as reconstructed by 3-D modeling, (2) outcrop edge of the Ellittico edifice (Branca, Coltelli, Groppelli, & Lentini, 2011), dashed where reconstructed, and (3) outcrop edge of the Mongibello volcano (Branca, Coltelli, Groppelli, & Lentini, 2011). (c) The 50 m equidistance contours map of the top of the sedimentary basement as reconstructed by Branca and Ferrara (2013) using boreholes and geophysical data (orange dots). (d) Schematic contour maps representing the paleo-morphology of the summit area of the Ellittico (1) and of the Valle del Bove (2) volcanic edifices, respectively, (from Branca, Coltelli, & Groppelli, 2011). (E) The 10 × 10 m cell size DTM of Mount Etna.

surfaces of the volcanic edifices were generated (Figure 3a). The workflow to create top and bottom surfaces was based on triangulated surfaces through which a number of mesh surfaces were generated by performing a Delaunay Triangulation algorithm from the points belonging to selected objects or vertices. Top surfaces of the Valle del Bove and Ellittico edifices resulted from the mosaicking of opportunely constructed meshes with those interpolated from available contours maps (Figure 3b1 and 2).

Since the exterior boundary faces of the triangulation generally form a convex hull of the point set, we used the polygonal curves bounding the domains (i.e., the outcropping limits of each volcanic system; see Figure 2b-1 to 3) to avoid this border effect clipping way (into ArcGis) the Delaunay triangles outside of curves previously converted into grids. Clipped grids were again imported into Move 3-D and used to generate volume of each volcanic system.

4. Volume Assessment and Eruption Rates

4.1. Volume Assessment

Once the top and bottom surfaces of the distinct volcanic edifices were obtained, volume generation was performed using the "create volume" tool of Move 3-D, which is able to produce a GeoCellular or TetraVolume between grid or mesh surfaces. Accordingly, we first calculated the total volume of Mount Etna by using the sedimentary substratum and the precollapse (i.e., before the summit collapse of Ellittico

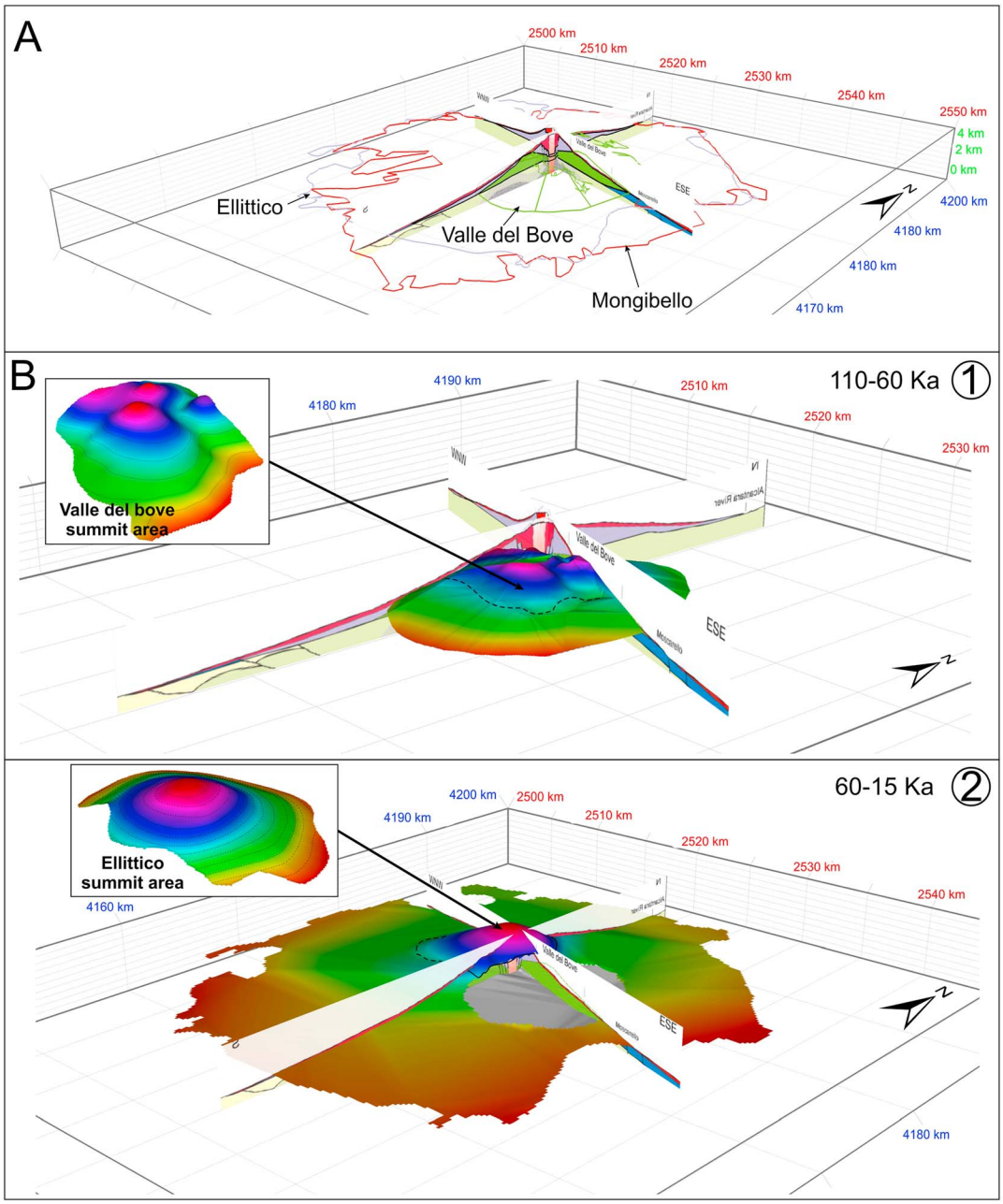

Figure 3. (a) Three-dimensional environment of Move software package showing the features of interest (lithological interfaces in the cross sections and boundaries in surface maps) converted into 3-D vector objects which have constituted the backbone of the model through which top and bottom surfaces of the volcanic edifices were generated. (b) 3-D view of mesh surfaces resulting from the interpolation of previously constructed reference lines: (1) top surface of the Valle del Bove edifice obtained by mosaicking the digital surface of its summit area (Figure 2d-2) with the opportunely constructed lower slope mesh surface and (2) top surface of the Ellittico edifice obtained by mosaicking the digital surface of its summit area (Figure 2d-1) with the lower slope mesh opportunely constructed.

volcano, occurred 15 ka ago, and the following formation of the Valle del Bove depression; see Figure 1a for location) paleo-topography as bottom and top grid surfaces, respectively. The precollapse morphology of Mount Etna is the result of the combination between the 10x10m cell size DTM of the modern topography and the grid surfaces representing the paleo-topography of the Ellittico and Valle del Bove volcanic edifices for the upper slopes (Branca, Coltelli, Groppelli, & Lentini, 2011; see Figure 2d) (Figure 3b-1 and 2). The interpolation of bottom (i.e., the sedimentary basement grid) and the so obtained combined top-

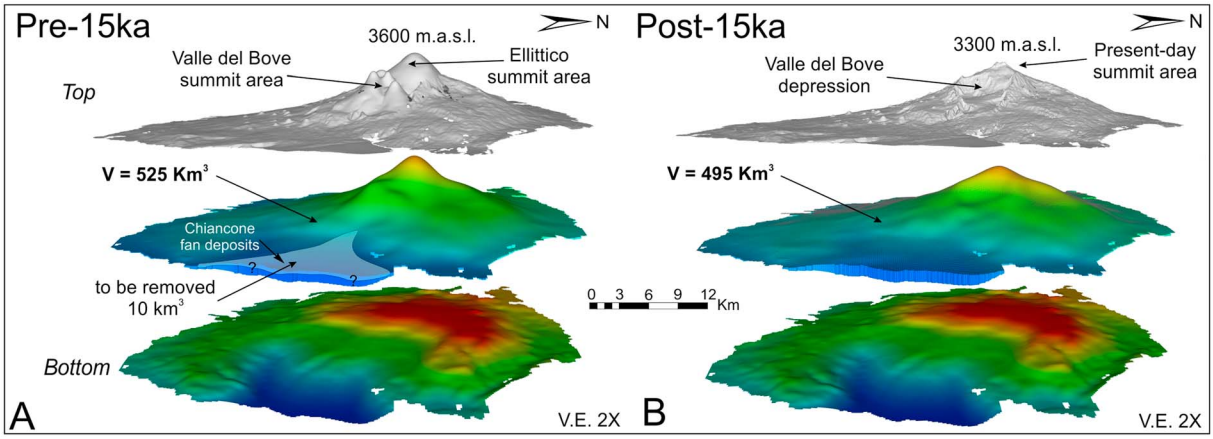

Figure 4. (a) Pre-15 ka (i.e., before the collapse of the Ellittico summit area and the Valle del Bove formation) volumetric model of Mount Etna (view from the sea) obtained by using as top-surface a new mesh surface generated by the combination of the paleo-topography of the Ellittico and Valle del Bove volcanic edifices and modern topography (10 × 10 m cell size digital terrain model). (b) Post-15 ka (i.e., after the collapse of Ellittico summit area and the Valle del Bove formation) volumetric model of Mount Etna. Each volume was obtained by using the "create volume tool" of Move software and by interpolating the respective top and bottom surfaces.

surface provides a total volume for the Mount Etna volcanic edifice of ~525 km^3 (Figure 4a). This volume should be corrected to ~545 km^3 by adding to it ~20 km^3 previously evaluated by Branca and Ferrara (2013) for the offshore area. According to previous authors (Calvari et al., 2004), about 10 km^3 of rocks were mobilized as a consequence of the formation of the Valle del Bove depression (about 10 ka ago; see Figure 1b) and deposited as debris avalanche deposit and detritic-alluvial body along the Ionian coast (Milo and Chiancone deposits; see Figure 1b). Since it was not possible to remove this rock volume from the precollapse volumetric model (Figure 4a), because no information is available on their bottom surface, we directly subtracted this volume (twice counted in Figure 4a) from the precollapse total volume, obtaining a corrected value of 535 km^3, which represents the actual volume of products emitted during the Mount Etna's volcanic phases.

Furthermore, by using the present-day volcano-tectonic configuration of Mount Etna (represented in the cross sections; Figure 2a) and its current topography (i.e., without Valle del Bove and Ellittico summit topography), we also evaluated the postcollapse volume of the volcano obtaining a value of ~495 km^3 (Figure 4b) corrected to ~515 km^3 by adding offshore volumes.

Since the Valle del Bove volcanic edifice lies both on the sedimentary substratum in the central part and above the Timpe lava shield in the eastern one (see cross sections in Figure 2a), its bottom surface was obtained by merging part of the grid-surface of the sedimentary substratum with a properly constructed Timpe top-surface. This interpolation allowed obtaining a volume of 102 km^3 (see Figure 5a). During the Ellittico volcano growth (<60 ka), the already emplaced Valle del Bove edifices constituted a morphological barrier, which hampered the expansion of the Ellittico volcanic products emitted by the summit vent southeastwards. Conversely, the occurrence of flank eruptions along the lower slopes of the Ellittico volcano allowed the lava flows to reach the Ionian coast (Branca, Coltelli, & Groppelli, 2011; Branca, Coltelli, Groppelli, & Lentini, 2011). This resulted in a complex 3-D reconstruction for the Ellittico edifice whereby we had to hole its modeled volume in the space occupied by the Valle del Bove edifices (196 km^3; see Figure 5b). By using the tectonostratigraphic setting provided by the cross sections (Figure 2a) and the paleo-topography of the Ellittico edifice (Figure 2d-1), we also obtained the postcollapse volume for this latter that resulted in 149 km^3. The difference between the precollapse (Figure 5d) and postcollapse configuration (Figure 5e) is therefore 46 km^3.

The modeled volume of the Mongibello edifice was estimated by considering as a bottom surface the post-15 ka top morphology of the Ellittico edifice reconstructed according to the cross sections (see above and Figure 2a). During the emplacement of the Mongibello volcano, remnants of the older edifices (Valle del Bove and Ellittico; see Figure 1b) in the eastern slope did not allow the lava flows to cover the area already occupied by them. This implied clipping the Mongibello volumetric model using the Ellittico volcano and

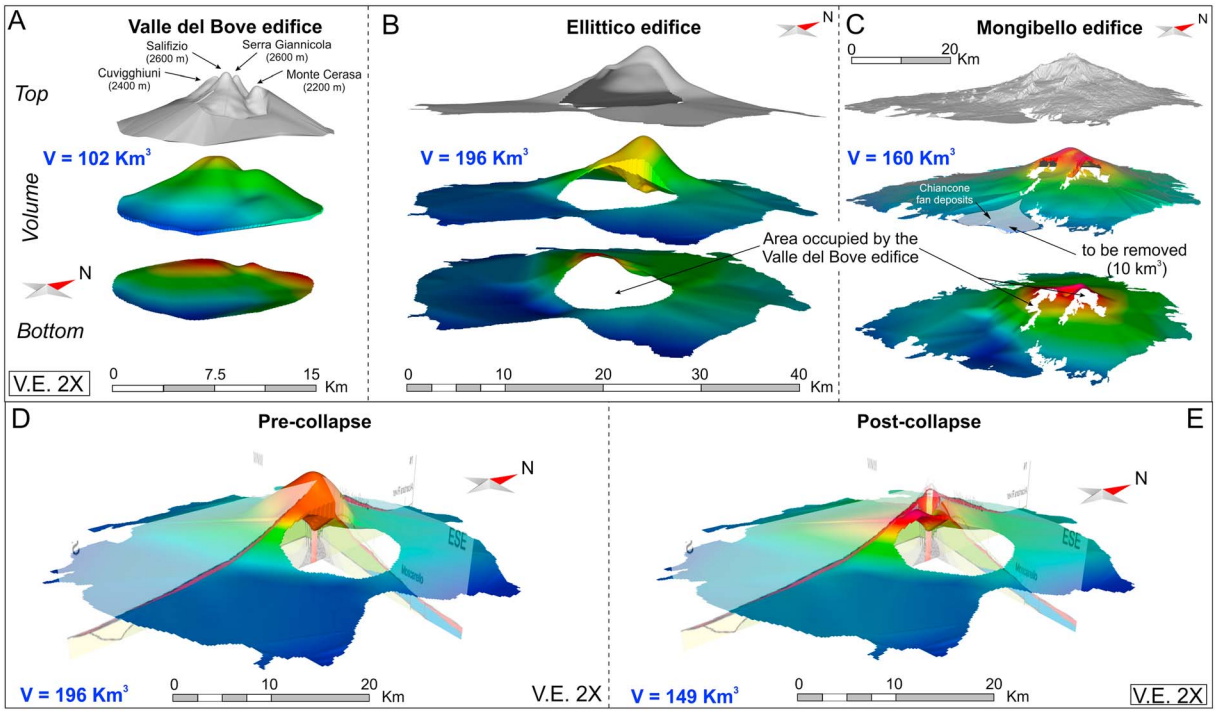

Figure 5. Volumetric models for the edifices that have formed during the main volcanic phases, that is, (a) Valle del Bove, and (b) Stratovolcano: Ellittico and (c) Mongibello. The difference between the Ellitico edifice in its (e) precollapse configuration and in its (d) postcollapse configuration reconstructed according to the available cross sections (in the background) is of 46 km ^{3}.

Valle del Bove edifices outcropping boundaries extracted from the geological map of Branca, Coltelli, Groppelli, and Lentini (2011), so resulting in 160 km^3 (see Figure 5c). This value should be further corrected by subtracting the ~10 km^3 of the Milo and Chiancone fan deposits (Figure 1b) that must be attributed to the Valle del Bove phase (see above).

Once top and bottom surfaces for each volcanic edifice were obtained, the subvolumes of Valle del Bove, Ellittico, and Mongibello edifices were determined by interpolating them (Figure 5), whereas the total volume (97 km^3) of the older edifices (i.e., Timpe and Basal Tholeiitic; see Figure 1b) was estimated through the difference between precollapse total volume of Mount Etna (535 km^3) and the sum of the volumes of Valle del Bove, Ellittico, and Mongibello volcanoes (448 km^3; see Table 2). Taking into account that about 4.5 km^3 was previously estimated by Branca and Ferrara (2013) for the subaerial lava flows of the Basal Tholeiitic phase, 83 km^3 (onshore + offshore products) has been attributed to the Timpe phase. The achieved subvolumes and associated errors (see section 4.1.1) are reported in the Tables 1 and 2 respectively (see below).

4.1.1. Reliability of the Model

To test the reliability of the model, we try to give a quantitative estimate of the error in calculated volumes even if it is difficult to be quantified being geological data heavily dependent from interpretation. However, among several sources of error, two main and sensitive types of uncertainty have been here considered: the accuracy in the altitude of the top of the basement and the geochronological dating.

Altitude of the top of the basement could be affected by a combination of errors related both to the interpolation method and the use of indirect subsurface data, for the latter estimated in 16% by Branca and Ferrara (2013).

Based on the distribution of the input raw data used to construct the top of basement (well-logs and geophysical surveys; Figure 2c), we derived a standard error map according to the ordinary kriging interpolation algorithm (Figure 6a). Elaboration shows that error potentially affecting the top of the basement increases moving toward the center of the volcano in agreement to the lacking of subsurface data in the summit area (Figure 2c). An averaged error in the interpolated altitude of ±25 m was computed. By pull down or up the top

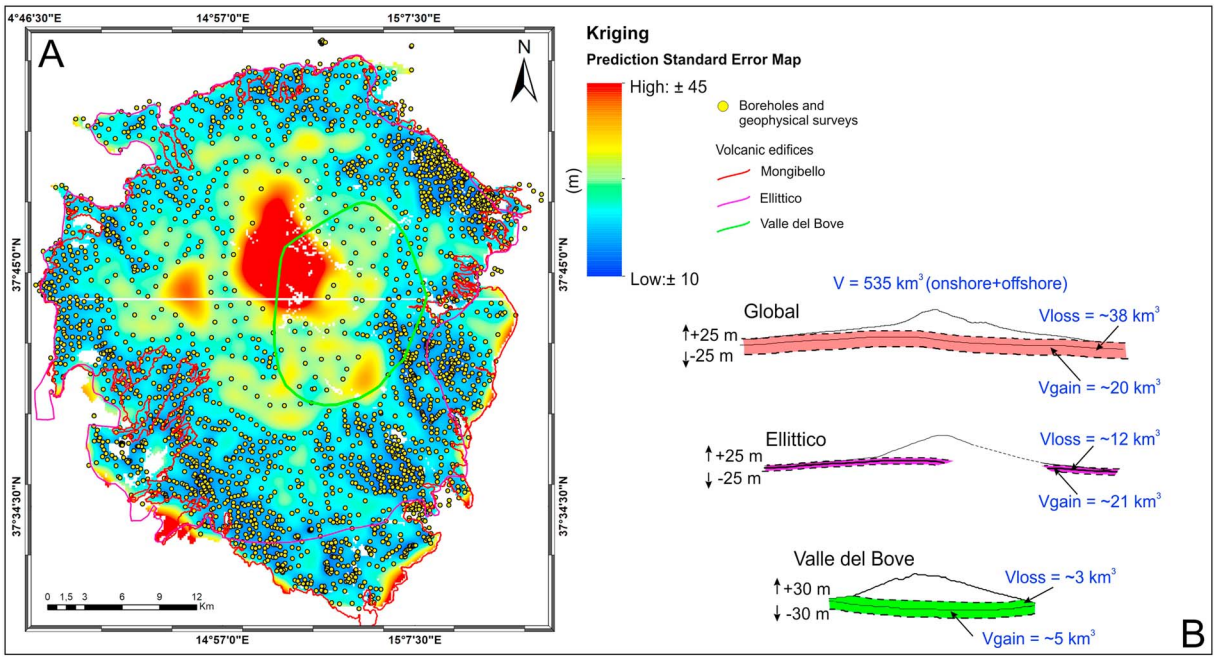

Figure 6. (a) Error estimation for the volumetric model obtained by using a standard error map for the depths of Etnean basement as derived from kriging interpolation (ArcGis platform). Map shows a potential error in the altitude of basements of ±25 m. This value was used to pull up and down the basement grid, which allow to estimate volume gain or loss for Mount Etna (global), Ellittico and Valle del Bove edifices, respectively. (b) Variation (gain-loss) in volume was then averaged and expressed in term of percentage of error (see Table 1) on the total and partial volumes. Further, obtained values were in turn averaged with error value previously estimate by Branca and Ferrara (2013) by comparing direct and indirect subsurface data.

of basement by this amount, an error in the Mount Etna global volume of ~5% (+30 and −28 km^3) can be estimated. Since it lies entirely on the basement too, we estimated the error in the volume for the Ellittico edifice in ~8% (+21 and −12 km^3) by using the same variation in altitude. We used instead an error in the depth of basement of ±30 m for the Valle del Bove because this value is the most represented altitude variation in the area occupied by the considered edifice (see Figure 6b) so obtaining an error in volume estimation of ~3.5% (±4 km^3).

By averaging errors coming from the two considered sources (interpolation method and the use of indirect subsurface data), a value of ±11%, ±12%, and ±10% has been estimated for Mount Etna global volume, Ellittico and Valle del Bove edifices, respectively. An error equal to that of Ellittico has been considered for the Mongibello phase because of their continuity, whereas averaged error for global volume has been considered for the Timpe phase (Table 1).

Finally, an error of the 8% in the age determination (see De Beni et al., 2011) was also considered.

By crosscutting the two kind of uncertainty, error range for eruption rates was estimated (see section 4.2 and Table 2).

As regard the possible loss of volume due to erosion, sparse pebbles of volcanic rocks within the alluvial sediments of major rivers surrounding the volcano suggest that, as a whole, a low rate of erosion affected the

Table 1
Percentage of Error in Volume Estimation for the Considered Volcanic Phases Obtained by Varying the Altitude of Basement Grid

Edifices	Volume (km^3)	Pull up (m)	New V1 (km^3)	Vloss (−)	Pull down (m)	New V2 (Km^3)	Vgain (+)	Error %	Error (%) by Branca and Ferrara (2013)	Averaged Error (%)
Mount Etna	535	25	497	38	−25	555	20	6	16	11
Timpe	83									11
Valle del Bove	102	30	99	3	-30	107	5	3.5	16	10
Ellittico	196	25	184	12	-25	217	21	8	16	12
Mongibello	150									12

Table 2
Tabulated Values of Achieved Partial Volumes of the Single Volcanic Phases and Related Time-Averaged Eruption Rates Calculated by Dividing the Emitted Volumes for the Duration of Emplacement of the Considered Volcanic Systems

Mount Etna total Volume (onshore + offshore) = 535 ± 59 km^3						
Volcanic phases		Volume (km^3)	Method	Time interval	Duration ±8%	Eruption rate (km^3/a)
Timpe		83 ± 9	by difference	220–110 ka	110 ka	7.54E − 04 ± 4.5%
Valle del Bove		102 ± 10	3-D modeling	110–60 ka	50 ka	2.00E − 03 ± 3.5%
Stratovolcano	Ellittico	196 ± 24	3-D modeling	60–15 ka	45 ka	4.3E − 03 ± 4.6%
	Mongibello	150 ± 17	3-D modeling	15 ka to present day	15 ka	1.00E − 02 ± 3%

Note. Note that by adding estimated errors (see Table 1) in volume and age determination, there is no significant variation in the final eruption rates.

Mount Etna during its lifetime. Large erosion was, on the contrary, experienced by Mount Etna occasionally, that is, during the Valle del Bove dismantling, a process that produced huge volume (~10 km^3; see Calvari et al., 2004) of detritic-alluvial sediments. The latter, known as Milo and Chiancone deposits (see Figure 1b for location), are currently preserved along the Ionian coast whereby they have been accounted in the volumetric model (see section 4.1).

4.2. Eruption Rates

Taking into account the previously estimated errors, time-averaged eruption rates were evaluated by dividing achieved volumes (total and partial) for the duration of emplacement of the considered volcanic systems (e.g., Branca & Ferrara, 2013). Accordingly, by dividing the total volume of Mount Etna (535 ± 59 km^3) for its duration (330 ± 8% ka), we obtained a global eruption rate of 1.6×10^{-3} ± 2.5% km^3/a. Partial volumes were instead divided for the relative time interval as provided by previous authors (e.g., De Beni et al., 2011) to obtain eruption rates for the considered volcanic phases.

As a whole, eruption rates of the single volcanic phases and related edifices increase constantly moving toward the present. In particular, the Timpe phase has the lowest value with an average eruption rate in the order of 10^{-4} ± 4.5% km^3/a. Eruption rate gradually increased in the interval 110–15 ka, during which it remained in the order of 10^{-3} km^3/a. In detail, we estimated an eruption rate of 2×10^{-3} ± 3.5% km^3/a for the Valle del Bove phase and 4.3×10^{-3} ± 4.6% km^3/a for the Ellittico volcano. Conversely, the Mongibello volcano (from 15 ka to present) has an eruption rate of 1×10^{-2} ± 3% km^3/a (see Table 2 and Figure 7).

5. Data Analysis

Computer-based geomodeling methods and tools enabled reconstructing a surface-based 3-D model of Mount Etna and of the distinct edifices related to its volcanic phases. Modeling was based on multisource geological and morphological data that were combined to comprehensively construct a geological body model of the volcano. Although any model is at best a simplified view of reality, the use of field and calibrated cross sections as reference objects, on which to build up the 3-D model, makes our results reasonable. However, some inconsistencies must be introduced in the final model since no boreholes have been drilled in the summit area of the volcano (see Figure 2c). As discussed above (section 4.1.1), this limitation adds an error in the volume measurements, which resulted particularly susceptible by the depth of the basement. By varying the altitude of the grid of the basement in the 3-D model (Figure 6b), an error in the range of 10–12% was estimated for the computed volumes, which means an error in the final eruption rates not exceeding the 5%.

A greater error should be instead considered when assessing volume coming from the difference between precollapse and postcollapse Ellittico configuration (Figures 5d and 5e) even if the interpreted geo-structural framework in the geological transects is coherent with models of caldera collapse (see Branca, Coltelli, & Groppelli, 2011; Branca, Coltelli, Groppelli, & Lentini, 2011; Monaco et al., 2010). However, other source of error such as the position of the buried contacts, amount of erosion, accuracy in the altitude of DTM, and its cell size resolution should be considered. Nevertheless, there is no significant variation to the final volcanic output rates, even considering an error in volumes estimation up to 20%.

A combination of the pre-15 ka paleo-topography of the summit area with the modern topography of the lower slopes (Figure 4a) gave us the opportunity of estimating the more reliable (i.e., before the collapse of Ellittico volcano and the formation of the Valle del Bove depression) global volume of Mount Etna (i.e., onshore + offshore), which resulted in ~535 km^3. The postcollapse global volume, estimated by using as top-surface only the modern topography (Figure 4b), is instead of about 515 km^3, a value that includes the Milo-Chiancone deposits. By subtracting the postcollapse configuration from the precollapse we obtained an unexpected difference of ~20 km^3. This value represents part of the volume resulting from the difference between the volumetric models obtained for the Ellittico in its precollapse and postcollapse configuration (Figures 5d and 5e). It could indicate the volume of rock ejected during the Plinian eruptions occurring at the end of Ellittico activity (between 15 ka and 15.5 ka, Coltelli et al., 2000), whose distal deposits were dispersed all over the central Mediterranean region including the Tyrrhenian and Adriatic seas, central Italy, and northern Libya (Albert et al., 2013; Del Carlo et al., 2017).

Evaluated global volume of Etna volcano (onshore + offshore) is, as expected, not far from that calculated by Branca and Ferrara (2013) since the same top and bottom surfaces were used. However, our 3-D modeling allows substantially redefining the partial volumes emitted during the considered volcanic phases as well as calculating the volumes of the Ellittico and of the Mongibello volcanoes (Stratovolcano phase; see Figure 1b).

6. Geodynamic Significance of the Increasing Eruption Rates

Since eruption rates might be influenced by several factors such as local crustal thickness, geodynamic setting, magma composition, and melt generation rate in the source region, we compared the Mount Etna output rates with those of other volcanoes located in different geodynamic settings in order to acquire information on possible changes of the aforementioned factors during the volcano's lifetime. Averaged eruption rates for different geodynamic settings were extracted from available data sets published by Crisp (1984) and White et al. (2006); we considered only those volcanic systems with comparable duration to that of Mount Etna.

Timpe and Valle del Bove phases are characterized by eruption rates in the order of 10^{-4} km^3/a, comparable with those of continental volcanic arc or volcanic field, whereas Stratovolcano phase (last 60 ka) has an averaged value of 7×10^{-3} km^3/a, 1 order greater than the previous rates and comparable with eruption rates of oceanic arc. Moreover, a drastic increase of emitted products in the last 15 ka, with a value of 1×10^{-2} km^3/a, has been evaluated. This aspect suggests that a significant change could have occurred in the source area and/or in the magma composition in addition to a stabilization of the plumbing system, favoring magma ascent (Branca, Coltelli, & Groppelli, 2011; Branca & Ferrara, 2013). According to Schiano et al. (2001), the geochemical evidence for a general transition from plume-type to arc-type mantle sources beneath Mount Etna could be related to the southward migration of subduction-related magmas along the Aeolian-Tindari-Letojanni Fault-System (ATLFS in Figure 1a where a vertical slab window occurs, see below) to interact with Etnean plume-related magmas or, alternatively, to the progressive shifting of the south-western lateral limit of the Ionian slab that could have juxtaposed the subduction zone and mantle plume, allowing their respective melts to provide the mixed-source magmas.

The lithosphere/asthenosphere system beneath the investigated area was thoroughly investigated through geophysical studies that highlighted the shape and geometry of the subducting Ionian slab (Figure 7a). In particular, some tomographic sections passing through the analyzed sector (Calò et al., 2012; Neri et al., 2009) suggest that a complete detachment of the Ionian oceanic slab has occurred north of Mount Etna. A high-velocity body, the detached portion of the slab originally separating the Aeolian magmatic province (subduction-related, calc-alkaline to shoshonitic volcanism; Peccerillo, 2005a) from the Etnean one (plume-related, mostly Na-alkaline volcanism; Corsaro & Pompilio, 2004), is currently sinking in the asthenosphere, lying beneath the western sector of the Aeolian Archipelago (Alicudi and Filicudi islands) at a depth of ~130 km (see Figure 8c). This accounts for trench-parallel slab breakoff and subduction cessation in the area with the consequent opening of a large and horizontal slab window right between the Etnean and Alicudi-Filicudi sectors (see also Barreca et al., 2016).

Many authors have debated the role of vertical slab windows in providing preferential pathways for the ascent and/or lateral migration of mantle melts (e.g., Etna and Vulture; Gvirtzman & Nur, 1999; Nicolich

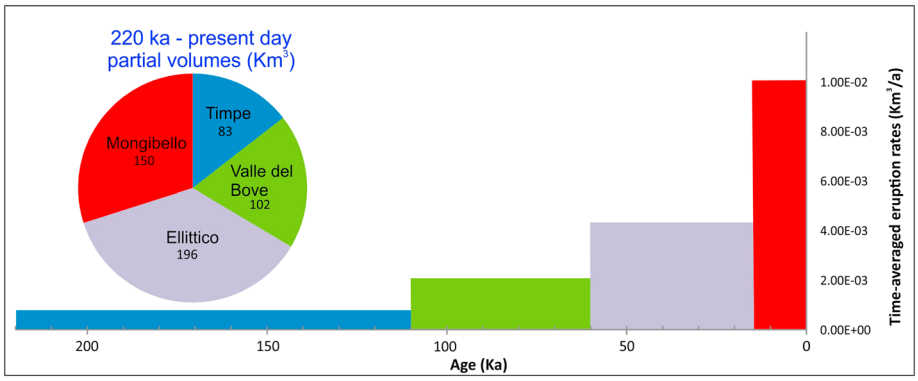

Figure 7. Graph showing the trend of eruption rates in the time interval 220 ka to present day.

et al., 2000; Doglioni et al., 2001; D'Orazio et al., 2007). Taking into account that along the Ionian-Calabrian subduction, the upper plate converges toward the lower plate slower than the subduction hinge (being W-directed; see Doglioni et al., 1999, 2009), giving rise to an upward flow of the asthenosphere in the hanging wall of the slab and to a much thicker asthenospheric mantle wedging, we suggest that also the horizontal window occurring in the subducting slab between the western Aeolian and the Etnean magmatic provinces could have given rise to mass transfer by thermal/density readjustment. According to this hypothesis, an originally hotter, fluid-rich, and less dense mantle wedge (i.e., the chemical and thermally modified European upper mantle; Figure 8a) was induced to flow laterally southward up to penetrating in the Etnean region since the Late Pleistocene (Figure 8b). This process was probably favored by mantel-crust decoupling (delamination) below the western sector of the Peloritani block. Influx of the European lithosphere/asthenosphere hot system above the colder and denser Africa-Ionian lithosphere is currently suggested by the trends of heat flow (Della Vedova et al., 2001) and of the regional Bouguer gravity anomalies in the area (Morelli, 1997). Immediately north of Mount Etna, along the Peloritani block (Figure 1a), a local maximum of heat flow (~100 mW/m^2) and a local minimum of Bouguer gravity anomaly (~50 mGal) occur (Figure 8b). Upwelling hot material in this sector could also have contributed to the substantial uplift of the Peloritani block (Barreca et al., 2016; Gvirtzman & Nur, 1999; Westaway, 1993), whereas mantle wedging beneath the Etnean sector could be evidenced by deep crustal compressive earthquakes currently occurring in the area (De Guidi et al., 2015; Lavecchia et al., 2007; Scarfì et al., 2016).

Further, by considering that (i) the onset of volcanism at the Aeolian Arc was around 1.3 Ma ago (Peccerillo, 2005b), (ii) volcanism cessation at its western sector (Alicudi and Filicudi) must not necessarily coincide with slab breakoff (a delay should be considered), and (iii) increasing of eruption rate at Mount Etna occurred about 60 ka ago, we retain that mantle migration started $<$1 Ma. Accordingly, taking into account a travelled distance of about 50 km (Figure 8b), this results on a velocity of the mantle flux of about 5 cm/a. This value could be consistent with the Calabrian trench migration rate during the Quaternary (Goes et al., 2004) even though the flux may have been locally accelerated by slab breakoff in the area.

7. Conclusions

Based on the digital reconstruction of a number of previously published thematic maps and data sets on the geological structure of Mount Etna, we provide for the first time a fairly consistent three-dimensional model of the volcano which has been built up into Move geomodeling software. 3-D modeling enables us to assess the volumes of volcanic products emitted during the main volcanic phases that have formed Mount Etna volcano. Above all, modeling allowed calculating for the first time the volumes emitted by the two most recently emplaced volcanoes, the Ellittico and Mongibello of the Stratovolcano phase (last 60 ka, see Figure 1b), that are about 350 km^3 of volcanic products, that is, ~ 60% of total volume of Mount Etna. In particular, ~196 km^3 were emitted during the growth of the Ellittico volcano (60–15 ka) and ~150 km^3 during the emplacement of the Mongibello volcano (15 ka to present day). This previously unresolved issue gives a more complete picture of the trend of eruption rates during the Mount Etna volcanic evolution, also highlighting a drastic

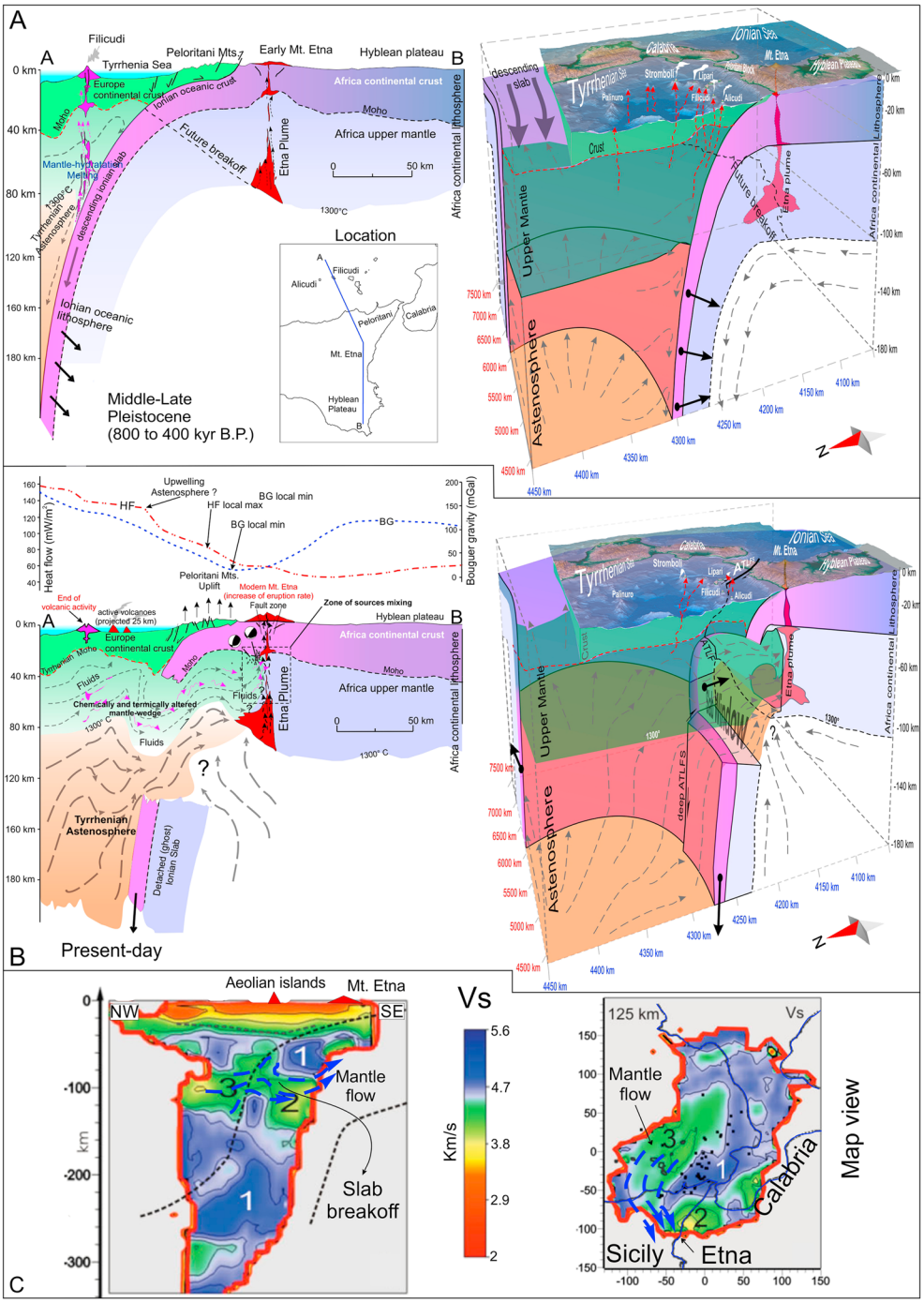

Figure 8. Schematic transects and 3-D -block models (perspective view from the NW) of the lithosphere/asthenosphere system beneath the Etna and western Aeolian arc regions reconstructed according to previously published geophysical studies (e.g., Brandmayr et al., 2010; Panza et al., 2007) and showing the possible geodynamic significance for the increasing of the eruption rate at Mount Etna since the last 60 ka. (a) During the Middle-Late Pleistocene, volcanism was still active in the western part of the Aeolian Arc (i.e., at Alicudi and Filicudi) implying that the Ionian slab was probably still continuous beneath the two volcanic islands. Suprasubduction mantle wedge was at that time chemically and thermally altered by fluids released from the descending slab. (b) The end of volcanic activity at Alicudi and Filicudi islands suggests the cessation of subduction in the area as a consequence of trench-parallel breakoff of the Ionian slab, a mechanism clearly depicted by tomographic images (Calò et al., 2012; see Figure 8c). Opening of a gateway into a slab originally separating the two lithosphere/asthenosphere systems with different densities and temperatures (i.e., Europe and Africa) and probably the nucleation of major oblique faults (i.e., ATLFS, IF, and NAF; see Figure 1a for location) at the edge of subduction system allowed the less dense, fluid-rich, and warmer suprasubduction mantle wedge to penetrate in the Etnean region. This process could explain the magma source mixing argued by previous authors and is supported by heat flow and gravity trends in the area, as well as by deep earthquakes with reverse mechanisms beneath the volcano (see Scarfì et al., 2016).

increase of emitted products in the last 15 ka with a value of 1×10^{-2} km^3/a (Figure 7). On average, eruption rates of Timpe and Valle del Bove phases are comparable with those of the continental volcanic field or continental arc, whereas the eruption rate of the Stratovolcano phase (Ellittico + Mongibello), in the order of 10^{-3} km^3/a, is almost similar to that of an island-arc volcanic system (see tables in Crisp, 1984, and White et al., 2006). Moreover, an estimated volume of about 20 km^3 has exceeded from the difference between the volume model reconstructed for the pre-15 ka Mount Etna (i.e., including the precollapse morphology of the Ellittico volcano) and that of the present-day volcano (Figure 4). In our opinion, this unrecovered rock volume has not fallen in the volcanic area but was probably dispersed in the neighboring areas.

Since Mount Etna volcano is situated on the Africa continental margin at the hinge of the subduction zone (Doglioni et al., 2001), anomalously high values of eruption rate, comparable with those of island-arc volcanoes, strongly support the hypothesis put forward by previous authors (e.g., Schiano et al., 2001; Tonarini et al., 2001), according to which a transition of Mount Etna products from a predominantly mantle-plume source to an island arc-type source (subduction-related) has occurred as a consequence of magmatic source mixing. Looking at the current geodynamic picture of this sector of eastern Mediterranean and considering tomographic images available for the area (Neri et al., 2009; Calò et al., 2012, Figure 8c), it is our opinion that trench-parallel breakoff of the Ionian slab north of Mount Etna (Barreca et al., 2016) has probably contributed to triggering the flow toward the south of a previously heated and fluids-enriched suprasubduction mantle wedge with consequent magmatic source mixing (i.e., arc-type versus plume-type) in the Mount Etna region. A similar geodynamic process, across vertical and/or horizontal slab windows, has been argued to explain magmatic source mixing in the southern Apennines (e.g., Mount Vulture volcano; see D'Orazio et al., 2007) and in the Kamchatka Peninsula along the western pacific subduction zone (see Manea & Manea, 2007). The flow of a metasomized mantle wedge toward the south is also expected from the polarized plate tectonic model (Doglioni & Panza, 2015) and by slab retreat dynamics (Doglioni et al., 2001) and clearly suggested in the area by available Vs models (Calò et al., 2012; see Figure 8c) that display a relatively low velocity body (i.e., the previously softened mantle wedge) penetrating through a horizontal slab window and wedging in the Etna sector. It is worth to note that the mantle flow direction (see 3-D block-model in Figure 8b) is suggested by the SKS fast wave polarization pattern in the area, which displays a sharp rotation from trench-parallel to trench-normal along the western sector of the Peloritani block (see Civello & Margheriti, 2004).

Clear effects of the inferred deep mixing process appear recorded by Mount Etna lava composition only recently (after 1970) with the emission of volcanics with a different geochemical signature to all previous historical products, being enriched in potassium and classified as K-trachybasalts (Corsaro & Cristofolini, 1996; Corsaro & Miraglia, 2014; Corsaro & Pompilio, 2004; Schiano et al., 2001).

Finally, volcanism cessation at Alicudi and Filicudi (~29 ka ago; see Lucchi, Santo, et al., 2013; Lucchi, Peccerillo, et al., 2013), the strong uplift of the Peloritani Block, the crustal shortening beneath Mount Etna volcanic edifice, and the increasing eruption rates at Mount Etna during the stratovolcano phase (since 60 ka ago onward), could be seen as the response to the Ionian slab breakoff in the area and the consequent flow toward the south of the suprasubduction mantle wedge and related island-arc magmatic source. This process frames well with the recent tectonic reorganization of the Nubia-Eurasia convergent boundary and the consequent onset of compression in the South-Tyrrhenian margin (Barreca et al., 2014; Billi et al., 2007, 2011).

Acknowledgments
S. Dominguez, J. Malavieille and A. Tibaldi are warmly acknowledged for their constructive comments and suggestions, which strongly improved the quality of the manuscript. All volumetric models are available in Move file format at the Open Science Framework general repository (https://osf.io), DOI: osf.io/4qbcz. Midland Valley Exploration Ltd is kindly acknowledged for providing Move 2017.2 geomodeling software package academic license.

References

Albert, P. G., Tomlinson, E. L., Lane, C. S., Wulf, S., Smith, V. C., Coltelli, M., et al. (2013). Late glacial explosive activity on Mount Etna: Implications for proximal–distal tephra correlations and the synchronisation of Mediterranean archives. *Journal of Volcanology and Geothermal Research*, *265*(2013), 9–26.

Aureli, A. (1973). Idrogeologia del fianco occidentale etneo. Atti 2° Convegno Internazionale sulle Acque Sotterranee, 28 Aprile-2 Maggio, Palermo.

Aureli, A., & Musarra, F. (1975). Idrogeologia del bacino del Fiume Alcantara (Sicilia). Atti 3° Convegno Internazionale sulle Acque Sotterranee (pp. 157–216). Palermo, 1–5 November.

Barreca, G., Bruno, V., Cultrera, F., Mattia, M., Monaco, C., & Scarfì, L. (2014). New insights in the geodynamics of the Lipari–Vulcano area (Aeolian Archipelago, southern Italy) from geological, geodetic and seismological data. *Journal of Geodynamics*, *82*, 150–167. https://doi.org/10.1016/j.jog.2014.07.003

Barreca, G., Scarfì, L., Cannavo, F., Koulakov, I., & Monaco, C. (2016). New structural and seismological evidence and interpretation of a lithospheric-scale shear zone at the southern edge of the Ionian subduction system (central-eastern Sicily, Italy). *Tectonics*, *35*, 1489–1505. https://doi.org/10.1002/2015TC004057

Billi, A., Faccenna, C., Bellier, O., Minelli, L., Neri, G., Piromallo, C., et al. (2011). Recent tectonic reorganization of the Nubia-Eurasia con-vergent boundary heading for the closure of the western Mediterranean. *Bulletin de la Societe Geologique de France*, *182*, 279–303.

Billi, A., Presti, D., Faccenna, C., Neri, G., & Orecchio, B. (2007). Seismotec-tonics of the Nubia plate compressive margin in the South-Tyrrhenian region, Italy: Clues for subduction inception. *Journal of Geophysical Research*, *112*, B08302. https://doi.org/10.1029/2006JB004837

Branca, S., Coltelli, M., De Beni, E., & Wijbrans, J. (2008). Geological evolution of Mount Etna volcano (Italy) from earliest products until the first central volcanism (between 500 and 100 ka ago) inferred from geochronological and stratigraphic data. *International Journal of Earth Sciences*, *97*, 135–152. https://doi.org/10.1007/s00531-006-0152-0

Branca, S., Coltelli, M., & Groppelli, G. (2011). Geological evolution of a complex basaltic stratovolcano: Mount Etna, Italy. *Italian Journal of Geosciences*, *130*(3), 306–317. https://doi.org/10.3301/IJG.2011.13

Branca, S., Coltelli, M., Groppelli, G., & Lentini, F. (2011). Geological map of Etna volcano, 1: 50,000 scale. *Italian Journal of Geosciences*, *130*(3), 265–291. https://doi.org/10.3301/IJG.2011.15

Branca, S., & Ferrara, V. (2013). The morphostructural setting of Mount Etna sedimentary basement (Italy): Implications for the geometry and volume of the volcano and its flank instability. *Tectonophysics*, *586*(2013), 46–64.

Brandmayr, E., Raykova, R., Zuri, M., Romanelli, F., Doglioni, C., & Panza, G. F. (2010). The lithosphere in Italy: Structure and seismicity. In M. Beltrando, et al. (Eds.), *Journal of the Virtual Explorer*, *36*, 1–73. https://doi.org/10.3809/jvirtex.2010.00224

Calò, M., Dorbath, C., Luzio, D., Rotolo, S. G., & D'Anna, G. (2012). Seismic velocity structures of southern Italy from tomographic imaging of the Ionian slab and petrological inferences. *Geophysical Journal International*. https://doi.org/10.1111/j.1365-246X.2012.05647.x

Calvari, S., & Groppelli, G. (1996). Relevance of the Chiancone volcanoclastic deposit in the recent history of Etna Volcano (Italy). *Journal of Volcanology and Geothermal Research*, *71*, 239–258.

Calvari, S., Tanner, L. H., Groppelli, G., & Norini, G. (2004). A comprehensive model for the opening of the Valle del Bove depression and hazard evaluation for the eastern flank of Etna volcano. In A. Bonaccorso, et al. (Eds.), *Etna Volcano Laboratory*, *Geophysical Monograph* (Vol. 143, pp. 65–75). Washington, DC: American Geophysical Union.

Calvari, S., Tanner, L. W., & Groppelli, G. (1998). Debris-avalanche deposits of the Milo Lahar sequence and the opening of the Valle del Bove on Etna volcano (Italy). *Journal of Volcanology and Geothermal Research*, *87*, 193–209.

Catalano, S., Torrisi, S., & Ferlito, C. (2004). The relationship between Late Quaternary deformation and volcanism of Mt. Etna (eastern Sicily): new evidence from the sedimentary substratum in the Catania region. *Journal of Volcanology and Geothermal Research*, *132*, 311–334.

Chiocci, L. F., Coltelli, M., Bosman, A., & Cavallaro, D. (2011). Continental margin large-scale instability controlling the flank sliding of Etna volcano. *Earth and Planetary Science Letters*, *305*, 57–64.

Civello, S., & Margheriti, L. (2004). Toroidal mantle flow around the Calabrian slab (Italy) from SKS splitting. *Geophysical Research Letters*, *31*, L10601. https://doi.org/10.1029/2004GL019607

Coltelli, M., Del Carlo, P., & Vezzoli, L. (2000). Stratigraphic constrains for explosive activity in the last 100 ka at Etna volcano. Italy. *International Journal of Earth Sciences*, *89*, 665–677.

Corsaro, R. A., & Cristofolini, R. (1996). Origin and differentiation of recent basaltic magmas from Mount Etna. *Mineralogy and Petrology*, *57*, 1–21.

Corsaro, R. A., & Miraglia, L. (2014). The transition from summit to flank activity at Mt. Etna, Sicily (Italy): Inferences from the petrology of products erupted in 2007–2009. *Journal of Volcanology and Geothermal Research*, *275*, 51–60. https://doi.org/10.1016/j.jvolgeores.2014.02.009

Corsaro, R. A., & Pompilio, M. (2004). Dynamics of magmas at Mount Etna. In A. Bonaccorso, et al. (Eds.), *Etna Volcano Laboratory*, *Geophysical Monograph* (Vol. 143, pp. 91–110). Washington DC: American Geophysical Union.

Crisp, J. A. (1984). Rates of magma emplacement and volcanic output. *Journal of Volcanology and Geothermal Research*, *20*, 177–211.

Cristallini, E. O., & Allmendinger, R. W. (2001). Pseudo 3-D modelling of Trishear Fault propagation folding. *Journal of Structural Geology*, *23*, 1889–1899.

Cultrera, F., Barreca, G., Burrato, P., Ferranti, L., Monaco, C., Passaro, S., et al. (2016). Active faulting and continental slope instability in the Gulf of Patti (Tyrrhenian side of NE Sicily, Italy): A field, marine and seismological joint analysis. *Natural Hazards*. https://doi.org/10.1007/s11069-016-2547-y

De Beni, E., Branca, S., Coltelli, M., Groppelli, G., & Wijbrans, J. (2011). $^{39}Ar/^{40}Ar$ isotopic dating of Etna volcanic succession. *Italian Journal of Geosciences*, *130*(3), 292–305.

De Guidi, G., Barberi, G., Barreca, G., Bruno, V., Cultrera, F., Grassi, S., et al. (2015). Geological, seismological and geodetic evidence of active thrusting and folding south of Mt. Etna (eastern Sicily): Revaluation of "seismic efficiency" of the Sicilian Basal Thrust. *Journal of Geodynamics*, *90*, 32–41. https://doi.org/10.1016/j.jog.2015.06.001

Del Carlo, P., Branca, S., & D'Oriano, C. (2017). New findings of Late Glacial Etna pumice fall deposits in NE Sicily and implications for distal tephra correlations in the Mediterranean area. *Bulletin of Volcanology*. https://doi.org/10.1007/s00445-017-1135-7

Della Vedova, B., Bellani, S., Pellis, G., & Squarci, P. (2001). Deep temperatures and surface heat flow distribution. In G. B. Vai & I. P. Martini (Eds.), *Anatomy of an Orogen: The Apennines and Adjacent Mediterranean Basins* (pp. 65–76). Dordrecht, Netherlands: Kluwer Academic.

Di Stefano, A., & Branca, S. (2002). Long-term uplift rate of the Etna volcano basement (Southern Italy) from biochronological data of the Pleistocene sediments. *Terra Nova*, *14*(1), 61–68.

Doglioni, C., Harabaglia, P., Merlini, S., Mongelli, F., Peccerillo, A., & Piromallo, C. (1999). Orogens and slabs vs their direction of subduction. *Earth Science Reviews*, *45*, 167–208.

Doglioni, C., Innocenti, F., & Mariotti, S. (2001). Why Mt. Etna? *Terra Nova*, *13*, 25–31.

Doglioni, C., & Panza, G. (2015). Polarized plate tectonics. *Advances in Geophysics*, 56. https://doi.org/10.1016/bs.agph.2014.12.001

Doglioni, C., Tonarini, S., & Innocenti, F. (2009). Mantle wedge asymmetries along opposite subduction zones. *Lithos*, *113*, 179e189. https://doi.org/10.1016/j.lithos.2009.01.012

D'Orazio, M., Innocenti, F., Tonarini, S., & Doglioni, C. (2007). Carbonatites in a subduction system: The Pleistocene alvikites from Mt. Vulture (southern Italy). *Lithos*, *98*(2007), 313–334.

Goes, S., Giardini, D., Jenny, S., Hollenstein, C., Kahle, H.-G., & Geiger, A. (2004). A recent reorganization in the south-central Mediterranean. *Earth and Planetary Science Letters*, *226*, 335–345. https://doi.org/10.1016/j.epsl.2004.07.038

Govers, R., & Wortel, M. J. R. (2005). Lithosphere tearing at STEP faults: Response to edges of subduction zones. *Earth and Planetary Science Letters*, *236*, 505–523.

Gutscher, M.-A., Dominguez, S., Mercier de Lepinay, B., Pinheiro, L., Babonneau, N., Cattaneo, A., et al. (2016). Tectonic expression of an active slab tear from high-resolution seismic and bathymetric data offshore Sicily (Ionian Sea). *Tectonics*, *34*, 39–54. https://doi.org/10.1002/2015TC003898

Gvirtzman, Z., & Nur, A. (1999). Formation of Mount Etna as a consequence of slab rollback. *Nature*, *401*, 782–785.
Kieffer, G. (1979). L'activité de l'Etna pendant les derniers 20000 ans. *Comptes Rendus de l' Academie des Sciences Paris*, *288D*, 1023–1026.
Lavecchia, G., Ferrarini, F., de Nardis, R., Visini, F., & Barbano, S. (2007). Active thrusting as a possible seismogenic source in Sicily (Southern Italy): some insights from integrated structural-kinematic and seismological data. *Tectonophysics*, *445*, 145–167.
Lo Giudice, E., Pandolfo, C., & Patanè, G. (1981). Dynamic evidence and hydrogeological implications of structures in recent volcanic areas. A multidisciplinary approach in the Etnean area. *Acqua-Aria*, *7*, 811–816.
Lucchi, F., Peccerillo, A., Tranne, C. A., Rossi, P. L., Frezzotti, M. L., & Donati, C. (2013). Volcanism, calderas and magmas of the Alicudi composite volcano (western Aeolian archipelago). *Geological Society, London, Memoirs*, *37*(2013), 83–111.
Lucchi, F., Santo, A. P., Tranne, C. A., Peccerillo, A., & Keller, J. (2013). Volcanism, magmatism, volcano-tectonics and sea-level fluctuations in the geological history of Filicudi (western Aeolian archipelago). *Geological Society, London, Memoirs*, *37*(2013), 113–153.
Manea, V. C., & Manea, M. (2007). Thermal models beneath Kamchaka and the Pacific plate rejuvenation from a mantle plume impact. In J. Eichelberger, et al. (Eds.), *Volcanism and subduction: The Kamchatka Region*, *American Geophysical Union Geophysical Monograph* (Vol. 172, pp. 77–90). Washington, DC: American Geophysical Union.
Monaco, C., De Guidi, G., & Ferlito, C. (2010). The morphotectonic map of Mt. Etna. *Bollettino della Società Geologica Italiana*, *129*(3), 408–428.
Morelli, C. (1997). The themes of crustal research in Italy and the role of the DSS-WA. *Seismics. Bollettino della Società Geologica Italiana*, *119*, 141–148.
Neri, G., Marotta, A. M., Orecchio, B., Presti, D., Totaro, C., Barzaghi, R., & Borghi, A. (2012). How lithospheric subduction changes along the Calabrian Arc in southern Italy: geophysical evidences. *International Journal of Earth Sciences (Geol Rundsch)*. https://doi.org/10.1007/s00531-012-0762-7
Neri, G., Orecchio, B., Totaro, C., Falcone, G., & Presti, D. (2009). Subduction beneath southern Italy close the ending: Results from seismic tomography. *Seismological Research Letters*, *80*, 63–70.
Neri, M., & Rossi, M. (2002). Geometria e volume dell'apparato vulcanico etneo: il contributo offerto dall'uso di mappe digitali. *Quaderni di Geofisica*, *20*, 1–16.
Nicolich, R., Laigle, M., Hirn, A., Cernobori, L., & Gallart, J. (2000). Crustal structure of the Ionian margin of Sicily: Etna volcano in the frame of regional evolution. *Tectonophysics*, *329*, 121–139. https://doi.org/10.1016/S0040-1951(00)00192-X
Nicolosi, I., D'Ajello Caracciolo, F., Branca, S., Ferlito, C., & Chiappini, M. (2016). The earliest open conduit eruptive center of the Etnean region: Evidence from aeromagnetic, geophysical, and geological data. *Bulletin of Volcanology*, *78*(50), 2–11. https://doi.org/10.1007/s00445-016-1042-3
Ogniben, L. (1966). Lineamenti idrogeologici dell'Etna. Rivista Mineralogica Siciliana
Palano, M., Ferranti, L., Monaco, C., Mattia, M., Aloisi, M., Bruno, V., et al. (2012). GPS velocity and strain fields in Sicily and southern Calabria, Italy: Updated geodetic constraints on tectonic block interaction in the central Mediterranean. *Journal of Geophysical Research*, *117*, B07401. https://doi.org/10.1029/2012JB009254
Panza, G. F., Peccerillo, A., Aoudia, A., & Farina, B. (2007). Geophysical and petrological modeling of the structure and composition of the crust and upper mantle in complex geodynamic settings: The Tyrrhenian Sea and surroundings. *Earth-Science Reviews*, *80*, 1–46.
Patella, D., & Quarto, R. (1987). Interpretation of shallow Schlumberger soundings in the western sector of Mt. Etna, Sicily. *Bollettino di Geofisica Teorica ed Applicata*, *XXIX*(II6), 309–320. XVII (N.100–102, 24.
Peccerillo, A. (2005a). *Plio–Quaternary Volcanism in Italy: Petrology, Geochemistry, Geodynamics* (365 pp.). Berlin: Springer.
Peccerillo, A. (2005b). The Aeolian arc. In A. Peccerillo (Ed.), *Plio-Quaternary Volcanism in Italy. Petrology, Geochemistry, Geodynamics* (pp. 173–213). Heidelberg: Springer.
Polonia, A., Torelli, L., Artoni, A., Carlini, M., Faccenna, C., Ferranti, L., et al. (2016). The Ionian and Alfeo-Etna fault zones: New segments of an evolving plate boundary in the central Mediterranean sea? *Tectonophysics*. https://doi.org/10.1016/j.tecto.2016.03.016
Rust, D., & Neri, M. (1996). The boundaries of large scale collapse on the flanks of Mount Etna, Sicily. In W. J. McGuire, A. P. Jones, & J. Neuberg (Eds.), *Volcano instability on the Earth and other Planets*. *Geological Society of London, Special Publication*, *110*, 193–208.
Sartori, R. (2003). The Tyrrhenian back-arc basin and subduction of the Ionian lithosphere. *Episodes*, *26*(3), 217–221.
Scarfì, L., Barberi, G., Musumeci, C., & Patanè, D. (2016). Seismotectonics of northeastern Sicily and southern Calabria (Italy): New constraints on the tectonic structures featuring in a crucial sector for the central Mediterranean geodynamics. *Tectonics*, *35*, 812–832. https://doi.org/10.1002/2015TC004022
Schiano, P., Clocchiatti, R., Ottolini, L., & Busa, T. (2001). Transition of Mount Etna lavas from a mantle-plume to an island-arc magmatic source. *Nature*, *412*, 900–903.
Tanguy, J. C. (1980). L'Etna etude petrologique et paleomagnetique: Implications volcanologiques (PhD thesis) (618 pp.). Univerity of Paris.
Tanguy, J. C., Condomines, M., & Kieffer, G. (1997). Evolution of the Mount Etna magma: constraints on the present feeding system and eruptive mechanism. *Journal of Volcanology and Geothermal Research*, *75*, 221–250.
Tonarini, S., Armienti, P., D'Orazio, M., & Innocenti, F. (2001). Subduction-like fluids in the genesis of Mt. Etna magmas: Evidences from boron isotopes and fluid mobile elements. *Earth and Planetary Science Letters*, *192*, 471–473.
Westaway, R. (1993). Quaternary uplift of southern Italy. *Journal of Geophysical Research*, *98*, 21,741–21,772. https://doi.org/10.1029/93JB01566
White, S. M., Crisp, J. A., & Spera, F. J. (2006). Long-term volumetric eruption rates and magma budgets. *Geochemistry, Geophysics, Geosystems*, *7*, Q03010. https://doi.org/10.1029/2005GC001002
Wilkerson, M. S., Medwedeff, D. A., & Marshak, S. (1991). Geometrical modelling of fault-related folds: A pseudo threedimensional approach. *Journal of Structural Geology*, *13*, 801–812.